Effect of short range ordering on the magnetism in disordered Fe:Al alloy

Tanmoy Ghosh [a], Ambika Prasad Jena [b], Biplab Sanyal [c], Hirosuke Sonomura [d], Takashi Fukuda [d], Tomoyuki Kakeshita [d], P.K. Mukhopadhyay [a,*], Abhijit Mookerjee [b]

[a] Laboratory for Condensed Matter Physics, Department of Condensed Matter Physics and Materials Sciences, S.N. Bose National Center for Basic Sciences, JD Block, Sector III, Salt Lake, Kolkata 700 098, India
[b] Department of Condensed Matter Physics and Materials Sciences, S.N. Bose National Center for Basic Sciences, JD Block, Sector III, Salt Lake, Kolkata 700 098, India
[c] Department of Physics and Astronomy, Uppsala University, Box 516, SE-75120 Uppsala, Sweden
[d] Department of Materials Science and Engineering, Graduate School of Engineering, Osaka University, 2-1, Yamada-oka Suita, Osaka 565-0871, Japan

A B S T R A C T

Magnetic behavior of equiatomic FeAl alloy is still not satisfactorily understood. In this work, we studied the magnetic properties of disordered FeAl alloy both experimentally and using first-principles theories and revisited the alloy system in perspective of the inhomogeneity present in the system. After obtaining magnetic exchange interactions from first-principles theories, we carried out Monte-Carlo simulations on special quasi-random structures (SQS) and compared the results with experimental measurements. We tried to understand the plethora of often differing results and explain them in terms of possible inhomogeneities in the system.

Keywords:
Transition metal alloy and compounds
Disordered systems
Short range ordering
Magnetization
Spin glasses
Electronic band structure

1. Introduction

Magnetic properties of disordered FeAl alloys have been studied extensively over the years. However, there does not seem to be a universally accepted understanding of the magnetic state and its ordering around the equiatomic composition. Magnetic moments of the Fe atoms in this alloy depend strongly on their local environments [1,2]. It is widely believed that ordered FeAl in the B2 structure is generally non-magnetic with a very small effective moment on the Fe atoms [2,3]. However, first-principles electronic structure calculations predict a ferromagnetic ground state [3,4]. Using LDA + U approach Mohn et al. [5] showed that for a range of U values this extra correlation leads to a non-magnetic ground state. This statement is true for a perfect B2 structure. However, if there is an anti-site defect in which a Fe atom sits on an Al site surrounded by eight Fe atoms, then this antisite Fe atom has a large local magnetic moment and polarizes other non-magnetic Fe atoms [3–10]. These anti-site defects are mainly responsible for the observed magnetization in B2 FeAl [4,11].

On the other hand, near the equiatomic composition disordered FeAl alloys have A2 type crystal structure and is probably a spin glass at low temperature [1,2,12–16]. First-principles density functional based calculations predict a ferromagnetic ground state with finite local moment on the Fe atoms [11]. Experimental measurements also report a finite local Fe magnetic moment with $m_{Fe} \approx 0.3\mu_B$ [1]. However, there are no general agreements on the transition temperature, magnetic moment and effective internal field [1,2,12,14–16] around the equiatomic composition. Experimental results vary widely from experiment to experiment. Possibility of non-collinear spin ordering has also been proposed in some literature [3,15]. In summary, magnetization of ordered B2 FeAl depends very much on the defect structures in the crystal, whereas magnetization in the disordered phase depends on the degree of disorder and atomic arrangements.

In this paper, we revisit the FeAl alloy both experimentally and theoretically and try to understand the plethora of often differing results and explain them in terms of possible inhomogeneities in the system. We prepared an FeAl alloy in the laboratory at equiatomic composition and carried out experiments to study the variation of magnetization with temperature. The alloy showed an initial transition to a spin glass like system with an interesting "anomalous" behavior at lower temperatures. The subsequent theory presented here is an effort to understand these experimental data. As the ground state is ordered, there is always a probability of finding some precipitated ordered clusters in the disordered background and such inhomogeneous disorder has been proposed earlier [1,2,17]. Therefore, the question we shall ask is, "what happens

* Corresponding author. Tel.: +91 33 23355706; fax: +91 33 23353477.
E-mail address: pkm@bose.res.in (P.K. Mukhopadhyay).

to the magnetic state when short range ordering or segregation is present in the sample?" Both magnetic moment and hyperfine field are sensitive to the defect structure and degree of disorder [4,16,18–20] and depend on the quenching procedure used to prepare the sample. In short, magnetic properties around this critical region are extremely sensitive to the structural phases present in the sample and the atomic ordering in the structure. The theoretical analysis will begin with the electronic structure and total energy calculations on the disordered alloy. The basic electronic structure method used here is the tight-binding linear muffin-tin orbitals (TB-LMTO) technique. Then we will calculate the exchange integrals from generalized perturbation theory using the orbital peeling technique [21] and use them for Monte Carlo (MC) simulations.

2. Experimental results

The sample was prepared near the equiatomic composition by arc melting high purity ($\geqslant$99.9%) Fe and Al pieces in a tri-arc furnace under argon atmosphere. Then it was vacuum annealed at 1000 °C for seven days followed by quenching into liquid N_2. Composition of the sample was checked using wavelength dispersive electron probe micro-analysis technique and obtained an average composition $Fe_{51.3}Al_{48.7}$ after measuring at five different spots on the sample with error in detection limit ≈0.02 wt-percent. For the XRD study, powder samples were prepared from the bulk ingot using a diamond file. XRD pattern was then taken using Mo Kα radiation in a laboratory powder diffractometer and is shown in Fig. 1. XRD pattern clearly shows the formation of the BCC crystal structure of FeAl alloy. However, along with the BCC FeAl the figure also depicts the presence of a superlattice (100) peak at $2\theta = 14^\circ$ and another (111) peak at $2\theta = 24.35^\circ$. These superlattice peaks indicate the formation and precipitation of ordered domains of B2 FeAl alloy. Formation of these types of superlattice peaks at higher Al concentration has also been reported earlier [1].

A few small pieces were cut from the sample ingot and taken for various magnetic measurements. Temperature dependent magnetization measurement in zero field cooled (ZFC) and field cooled (FC) protocols were performed in a Quantum Design™ SQUID magnetometer. We used a Quantum Design PPMS® system for frequency dependent susceptibility measurements. Results of these measurements are shown in Fig. 2. ZFC and FC magnetization data at $H = 25$ Oe are taken from the work of Mukhopadhyay et al. [22]. As the sample was cooled down from room temperature, magnetization continued to increase till a rounded peak appeared around temperature T_f. In magnetization measured at $H = 25$ Oe ZFC and FC curves started bifurcating around 250 K which is far above T_f, whereas there was no bifurcation between them till T_f in magnetization measured at $H = 100$ Oe. Bifurcation between ZFC and FC magnetizations at this rather high temperature and low field could be due to the inhomogeneous nature of the sample. In magnetization measured at $H = 25$ Oe T_f was approximately at 55 K, whereas at $H = 100$ Oe T_f shifted down to approximately at 35.5 K. This signifies that the peak was very sensitive to the applied magnetic field and drastically shifted to a lower temperature region as the magnetic field was increased. Below T_f, magnetization started to decrease and there was a further significant bifurcation between the ZFC and FC magnetizations similar to those of a spin glass system. Frequency dependent a.c. susceptibility measurements, shown in Fig. 2 (right panel), indicated that this peak was also sensitive to the frequency of the applied a.c. field. We found $\phi\ (= \Delta T_f/(T_f \Delta log f)$, where

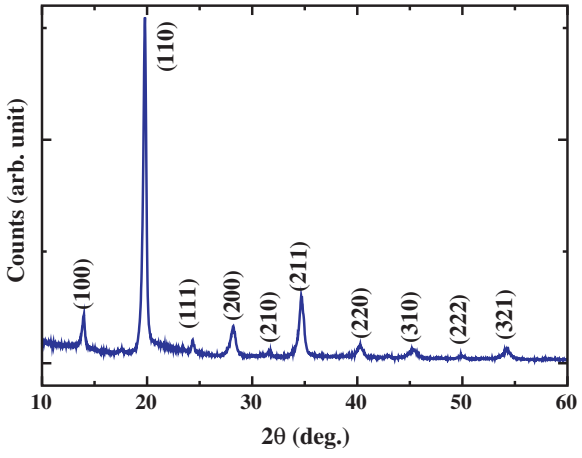

Fig. 1. Room temperature XRD pattern measured using Mo Kα radiation.

f is the frequency of the applied signal), which is a quantitative measure of shift of T_f per decade of frequency, is 0.005. This value of ϕ is similar to those of a canonical metallic spin glass system. Consequently we propose that this was spin glass transition. We shall see from the subsequent theoretical investigations that this spin glass behavior came from the frustration produced by the fluctuating exchange energy in the disordered structure and the decrease in magnetization below T_f was due to the gradual thermal freezing of the magnetic moments.

As the temperature was lowered further, around temperature T_a magnetization showed a dip followed by an upturn. For the case of magnetization measured at $H = 25$ Oe, $T_a^{ZFC} \approx 16$ K and $T_a^{FC} \approx 25$ K. At a higher magnetic field $H = 100$ Oe, almost same behavior was retained by both the ZFC and FC magnetizations. FC magnetization became flat below T_f followed by the upturn, but now the dip was drastically decreased. At $H = 100$ Oe, $T_a^{ZFC} \approx 20$ K and this shows that T_a moved to a higher temperature region as the field was increased. In frequency dependent a.c. susceptibility measurements, we found that T_a was also insensitive to the frequency of the applied signal (as shown in the right panel of Fig. 2). Similar anomalous upturn in magnetization was reported earlier by Nigam et al. in the disordered AuCr system [23]. They attributed this upturn to ferromagnetic moments formed during field cooling. In our sample formation of some short-ranged ordered clusters is evident from the XRD pattern. As a result, the total magnetization of the sample had two components' contributions, one coming from the ordered clusters and another from the disordered structure which in-turn became a spin glass at lower temperatures. The ordered clusters were paramagnetic with $1/T$ (Curie) magnetization dependence while below the spin glass transition temperature (T_f), the spin glass component decreased due to gradual freezing of clusters. At low enough temperature the paramagnetic component became dominant and caused the upturn in magnetization. As the external magnetic field was increased, below T_f, the paramagnetic contribution became stronger than the spin glass contribution, and pushed T_a towards the higher temperature region. It is also well known that in spin glasses T_f decreases as the applied magnetic field increases. Therefore, with increasing magnetic field T_f and T_a move in the opposite direction to each other and would eventually destroy the peak and dip in magnetization curve. This explains why the curve was flat below T_f in FC magnetization measured at $H = 100$ Oe and we will look more into this feature in our subsequent theoretical analysis.

3. Theoretical investigations

In the remaining part of this communication, we will to analyze and understand the experimental data from a density functional based ab initio electronic structure calculation supplemented with Monte Carlo simulations. Our emphasis is to build a theoretical understanding through a rigorous and parameter free first-principles theory.

3.1. Electronic structure calculations

We shall begin our theoretical investigations with an electronic structure determination of the valence electrons of FeAl. The disorder fluctuations in the alloy are local. Therefore, a tight-binding basis will be most suitable in describing such disorder. We shall choose the tight-binding linear muffin-tin orbitals technique (TB-LMTO) [24] as our basic methodology. There are powerful mean-field theories available to describe the disorder, like the coherent potential approximation (CPA). However, such single site approximations cannot deal with inhomogeneities like short-ranged ordering or clustering. We have the choice of four successful generalizations: three of which are based on the augmented space theorem introduced by one of us, Mookerjee [25,26]: the itinerant cluster approximation (ICA) [27], the traveling cluster approximation (TCA) [28] and the augmented space recursion (ASR) [29]. We also have the special quasi-random systems (SQS) introduced by Zunger et al. [30]. Mention must also be made of the gamma expansion method [31,32]. In this communication we have chosen the ASR and SQS, making use of the self-consistent ASR codes developed by Mookerjee and his group [29].

The species and spin projected density of states is shown the left panel of Fig. 3. The density of states is dominated by the relatively localized d-electrons of Fe, with the more itinerant p-electrons of Al contribute the base. The alloy is magnetic, and the magnetization density integrated over the atomic sphere provides the moments associated with each sphere.

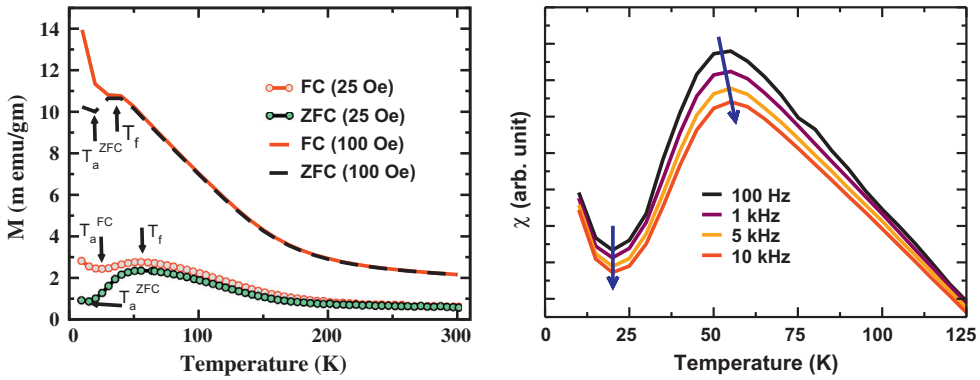

Fig. 2. (Left panel) Temperature dependent magnetization in ZFC and FC modes and at different applied field. (Right panel) Frequency dependent a.c. susceptibility as a function of temperature.

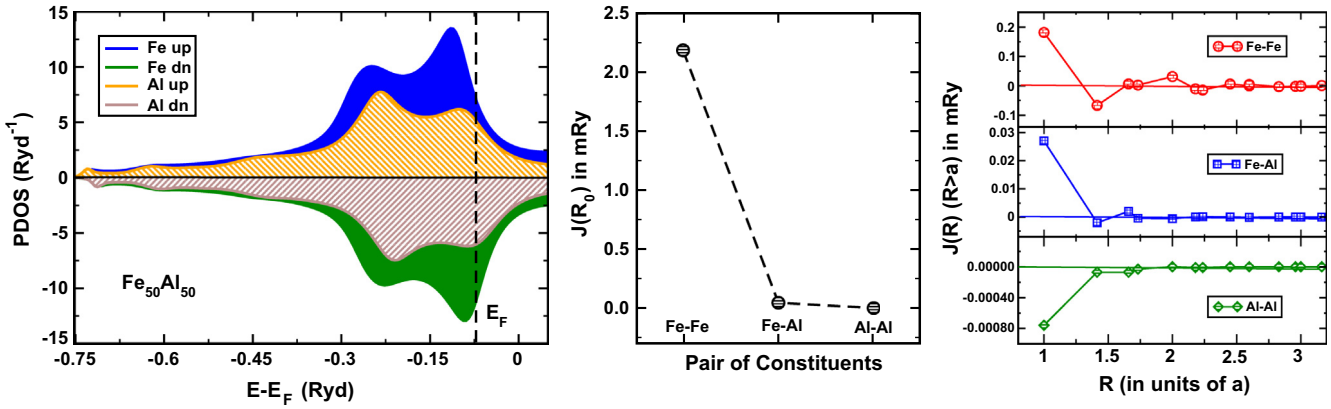

Fig. 3. The spin-projected density of states for FeAl, projected on Fe and Al atoms are shown in the left panel. The magnetic exchange energies for Fe–Fe, Fe–Al and Al–Al pairs are shown in central panel (for the dominant nearest neighbor exchanges) and right panel (for the other neighbors).

3.2. Magnetic exchange interactions

Once the formation of a magnetic moment within an atomic sphere (AS) is understood using the TB-LMTO-ASR as described above, the next step is to understand how these moment-carrying AS-s order. The moment formation is an itinerant electron picture in which the moment is produced by an exchange splitting of the majority and minority spin projected densities of states. The ordering of these AS is studied here via the derivation of the lowest configurational energy for a specified moment configuration. We shall start with the disordered phase and set up a perturbation in the form of local concentration fluctuations associated with an ordered phase and study whether the alloy can sustain such a perturbation. This approach includes the generalized perturbation method (GPM) [33] which we shall follow in this work.

We shall introduce *occupation* variable $n_{\vec{R}_i}$ which takes the value 0 or 1 according to whether the AS labeled by $\vec{R}_i$, occupied by a Fe atom, carries up or down magnetic moments. In the paramagnetic phase when the AS carrying up and down moments are arranged randomly, the fluctuations $\delta n_{\vec{R}_i} = n_{\vec{R}_i} - \langle n_{\vec{R}_i} \rangle = \pm 1/2$ and $\langle \delta n_{\vec{R}_i} \rangle = 0$. The generalized perturbation approach expands the energy in this new configuration about the energy of a perfectly disordered state:

$$E = E^{(0)} + \sum_{\vec{R}_i} E^{(1)}_{\vec{R}_i} \delta n_{\vec{R}_i} + \frac{1}{2} \sum_{\vec{R}_i,\vec{R}_j} E^{(2)}_{\vec{R}_i,\vec{R}_j} \delta n_{\vec{R}_i} \delta n_{\vec{R}_j} + \cdots \quad (1)$$

The coefficients $E^{(0)}$, $E^{(1)}_{\vec{R}_i}$, ... are the cluster interactions. $E^{(0)}$ is the averaged total energy of the paramagnetic pattern. $E^{(1)}_{\vec{R}_i}$ is the energy change if we replace an A atom by a B atom in the disordered background. This 'on-site energy' is unimportant for homogeneous bulk magnetic order emerging from disorder. The pair interactions $E^{(2)}_{\vec{R}_i,\vec{R}_j} = E^{AA}_{R_iR_j} + E^{BB}_{R_iR_j} - 2E^{AB}_{R_iR_j}$ are the important energies governing the emergence of bulk magnetism. Further, the fourth term onwards in the series can be neglected since in most cases the coefficients are progressively small. This maps the problem of magnetic ordering onto a classical Ising model:

$$\Delta E = H = -\frac{1}{2} \sum_{\vec{R}_i,Q} \sum_{\vec{R}_j,Q'} J^{QQ'}(|\vec{R}_i - \vec{R}_j|) S_{\vec{R}_i} S_{\vec{R}_j}. \quad (2)$$

The variables $S_{\vec{R}_i}$ are now classical variables taking values ±1. Q, Q' refer to species Fe and Al and $J^{QQ'}(|\vec{R}_i - \vec{R}_j|) = -\frac{1}{4} E^{(2)}_{\vec{R}_i,\vec{R}_j}$. Since $J^{QQ'}(|\vec{R}_i - \vec{R}_j|)$ are very small energy differences of large individual energies and a separate calculation of each component produces errors larger than the small differences themselves, these interatomic 'pair-exchange' parameters were calculated using orbital peeling technique [21,34]. The details of the method has been described in Ref. [34]. Fig. 3 (center and right panel) shows the exchange energies as functions of neighbor distance. We first note that the exchange energies are dominated by the Fe–Fe exchange. The Fe–Fe exchange is long ranged and oscillatory rather similar to a RKKY interaction, rapidly decaying due to disordered scattering.

Such an oscillatory exchange leads to frustration and the possibility of a low temperature spin glass phase.

3.3. Monte Carlo simulations

To study the temperature dependence of the magnetization, we carried out Monte Carlo simulations on both the ordered B2 and disordered A2 FeAl system. The random structure for the disordered FeAl has been generated by two different methods: (i) by random structures generated from random occupancy of lattice sites, and (ii) by SQS, representing the random structure. Magnetic exchange interaction for ordered B2 structure is taken same as that of the disordered structure.

The idea of SQS has been introduced by Zunger et al. [30]. The authors showed that these SQS super cells mimic, even for small sizes ($N = 8$ atoms, for example), the first few physically most relevant radial correlation functions either of a perfectly random atomic arrangement or arrangements with short-ranged ordering far better than standard random structures generated by producing random occupation variables on the underlying lattice.

The method of generation of the SQS has been described in detail by von Pezold et al. [35]. Any given configuration σ of A and B components is discretized into "figures" $f(k, m)$, where the figure has k vertices separated by m-th neighbor distance. With each vertex i we associate occupation variables n_i, which take the values ±1 according to whether the site i is occupied by A or B atom. We place the figure $f(k, m)$ at the location J on the lattice and define $\Pi_{f(k,m)}(J, \sigma)$ as $\prod n_i$. If there are $D_{f(k,m)}$ figures per site, then the lattice average is defined as:

$$\bar{\Pi}_{f(k,m)}(\sigma) = \frac{1}{ND_{f(k,m)}} \sum_{J} \Pi_{f(k,m)}(J, \sigma). \tag{3}$$

The configuration averaged physical property is given rigorously as:

$$\langle Q \rangle = \sum_{f(k,m)} D_{f(k,m)} \bar{\Pi}_{f(k,m)} p_{k,m}. \tag{4}$$

The $N\prime$ values of $p_{k,m}$ are deduced from above if we can calculate $N\prime$ values of $\langle Q \rangle$. Zunger et al.'s main idea was that instead of calculating $\bar{\Pi}_{f(k,m)}$ by statistical sampling methods, one may design special N-atom periodic structures S whose distinct correlation functions $\bar{\Pi}_{f(k,m)}(S)$ best match the configuration averaged $\langle \bar{\Pi}_{f(k,m)} \rangle$. The short-ranged order may be built into the calculated configuration averages and thus affect the generation of the SQS. Instead of taking average over many configurations, SQS allows us to do Monte Carlo simulation on a single configuration designed by considering all the correlation functions. This method is therefore computationally much faster than those that rely on configurational averaging.

Monte-Carlo simulations were carried out using Metropolis algorithm with single spin flip dynamics. Simulations were performed with 250,000 MC steps and measurements were done after skipping 25,000 steps to reach equilibrium.

Temperature dependent magnetization of the ordered structure of B2 FeAl alloy, obtained from MC simulation, is shown in the left panel of Fig. 4 (black line). This result confirms that perfectly ordered structure of FeAl alloy is paramagnetic as also predicted by first-principles density functional theories [3,4,6], followed by a ferromagnetic transition at very low temperature. This magnetic transition is approximately at the same temperature T_a^{ZFC} where we found the anomalous upturn in ZFC magnetization ($H = 25$ Oe). The blue line in the figure (left panel of Fig. 4) shows the temperature dependence of magnetization in disordered FeAl alloy obtained from MC simulation with SQS. MC simulated magnetic susceptibilities of disordered FeAl alloy, both with random structure and SQS representing the disordered structure, are shown in the right panel of Fig. 4 and it shows that results in both the cases agree fairly well. Therefore, if not otherwise mentioned, for the MC simulations in disordered structure presented in the remaining part of this paper were done with SQS's as MC simulations are computationally much faster than with random structures. The simulated magnetization leads to a paramagnetic to ferromagnetic transition temperatures (T_C) approximately at 250 K (characteristic peak in the susceptibility graph as shown in the right panel of Fig. 4) which is higher than our experimental data. However, our experimentally prepared sample contains a significant amount of ordered clusters and the presence of these ordered clusters may have affected the magnetic transition temperatures in the sample. We shall explicitly show this later. The interesting part still to be explained is the low temperature structures in magnetization and the contradictory results quoted by different experimentalists.

Disordered FeAl has a tendency towards forming into an inhomogeneous alloy and the degree of inhomogeneity depends on the preparation and annealing procedures followed to prepare the sample. Therefore, the question now is – does the magnetic transition temperature and magnetization behavior depend strongly on the inhomogeneity present in the sample? If so, this would explain why results vary from experiment to experiment. This in turn would explain the variety of experimental results measured on essentially different samples.

A crude approach to find out the effect of ordered clusters on the magnetization is to assume that there is no correlation between the precipitated ordered clusters and the disordered background. Then the total magnetization is a proportional mixture of the two phases and is given by

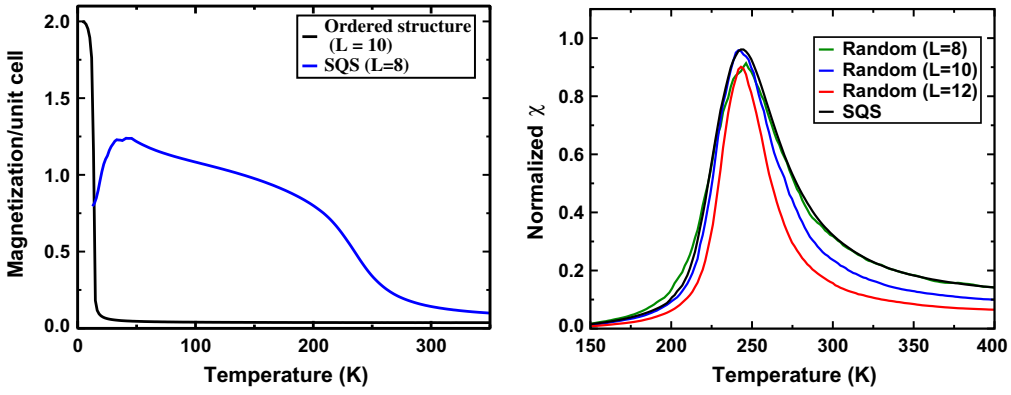

Fig. 4. (Left panel) Variation of magnetization with temperature obtained from MC simulations. In the graph, the black line represents an ordered structure of B2 FeAl alloy and the blue line is for SQS representing a perfectly random structure of disordered FeAl alloy. The structures are body-entered cubic with volume $[(L-1)a]^3$ where a is interatomic distance along the cube sides. (Right panel) Normalized susceptibility obtained from MC simulation on SQS and random structures representing disordered FeAl alloy. (For interpretation of the references to colour in this figure legend, the reader is referred to the web version of this article.)

$$M_{\text{total}} = xM_{\text{ord}} + (1-x)M_{\text{disord}}. \quad (5)$$

Variation of M_{total} with temperature, obtained from MC simulation, is shown in Fig. 5. The intermediate portion between T_C and T_f agrees well with the experimentally observed magnetization i.e. magnetization of the inhomogeneous sample. This model also successfully reproduces the region near T_a showing that anomalous upturn is due to the magnetic response of the ordered clusters. However, the region near T_C is not very satisfactory, specially the variation of T_C with the ratio of ordered and disordered structure. The probable reason for failure of this model near T_C is that in this model there is no correlation between the ordered and disordered structures and consequently one does not affect the behavior of other.

We can now try to understand the experimentally observed magnetization behavior more accurately by studying an inherently inhomogeneous disordered structure. Our Monte-Carlo simulation based on SQS structure allows us to introduce short range ordering and clustering in a controlled manner. Here we designed SQS structures according to different values of Warren-Cowley short range order parameter ($\alpha > 0$ indicates clustering (clusters formed by like atoms) while $\alpha < 0$ leads to short-ranged ordering which is relevant to this study).

The results of the MC simulations involving inhomogeneous disorders are shown in Fig. 6 and it shows that our simulation has nicely reproduced the experimentally observed temperature dependent magnetization behavior. The right panel of Fig. 6 shows the variation of transition temperature T_C with the variation of short range order parameter α and depicts that T_C varies almost linearly with α. As the system moves from the state of clustering to the state of short-ranged ordering through a perfectly disordered state, T_C decreases continuously. As mentioned above, experimentally prepared samples contain inhomogeneity and the inhomogeneity content may vary from sample to sample depending upon the preparation and annealing procedures. This gives an explanation of why transition temperature varies widely in different experimentally reported results. Fig. 6 (left panel) shows that in both the homogeneously and inhomogeneously disordered sample magnetization decreases below temperature T_f. Therefore, the spin glass phase transition is a property of the disordered phase and comes due the long ranged oscillatory magnetic exchange interaction present in the alloy. However, the figure (left panel of Fig. 6) depicts that the anomalous upturn in magnetization below T_a is present only in the inhomogeneously disordered samples with short-ranged ordering (negative values of α). This confirms that the upturn in magnetization below T_a comes from the short-ranged ordering present in the sample.

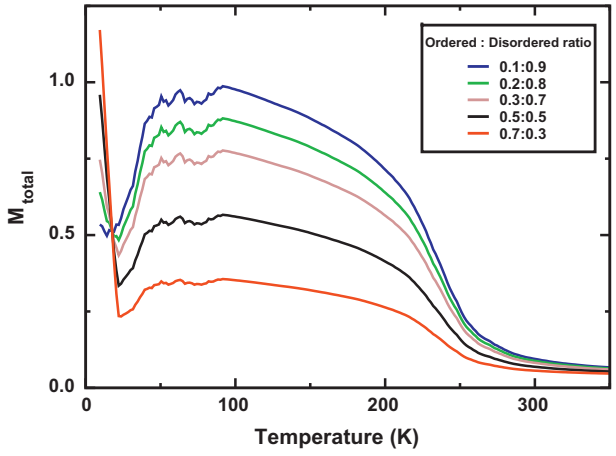

Fig. 5. Independent mixtures of ordered and disordered structures (from top to bottom with increasing ordering fraction).

3.4. Effect of external magnetic field

In the experimental section, it has been shown that external magnetic field drastically changes the magnetization behavior of disordered FeAl alloy and the peaks in the magnetization curve could be washed away by applying sufficiently high magnetic field. We therefore carried out MC simulations in presence of an external magnetic field and investigated how that affects magnetization behavior and transition temperatures.

In presence of an externally applied magnetic field h, Hamiltonian of Eq. 2 becomes:

$$\Delta E = H = -\frac{1}{2}\sum_{\vec{R}_i,Q}\sum_{\vec{R}_j,Q'} J^{QQ'}(|\vec{R}_i - \vec{R}_j|)S_{\vec{R}_i}S_{\vec{R}_j} - h\sum_{\vec{R}_i} S_{\vec{R}_i}. \quad (6)$$

Simulations have been done for different values of h. Effect of external magnetic field on the ordered B2 FeAl is shown in the left panel of Fig. 7. Magnetization of the ordered structure increases with the increase in magnetic field as more and more spins get oriented towards the field direction. In case of homogeneously disordered structure, along with the increase in magnetization (shown in the central panel of Fig. 7) T_f shifts towards lower temperature similar to our experimental observation. Effect of external magnetic field on the structures having short range ordering is shown in the right panel of Fig. 7 and it confirms the experimental observation that the peaks in the magnetization curve were getting destroyed with the increase in magnetic field. At higher magnetic field, magnetic

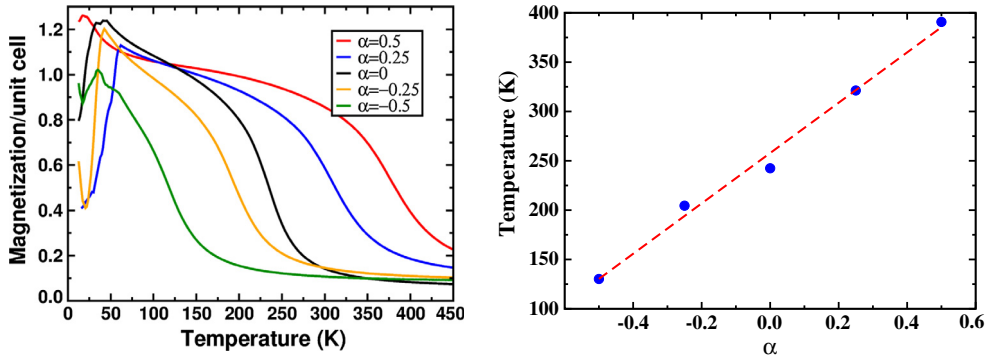

Fig. 6. (Left panel) Effect of short-ranged ordering and clustering on the magnetization. Temperature dependent magnetizations are obtained from MC simulation on SQS with different kind of inhomogeneities and for different values of α. (Right panel) Variation of T_C with short range order parameter α. The dashed line is given as guide to the eye for a straight line.

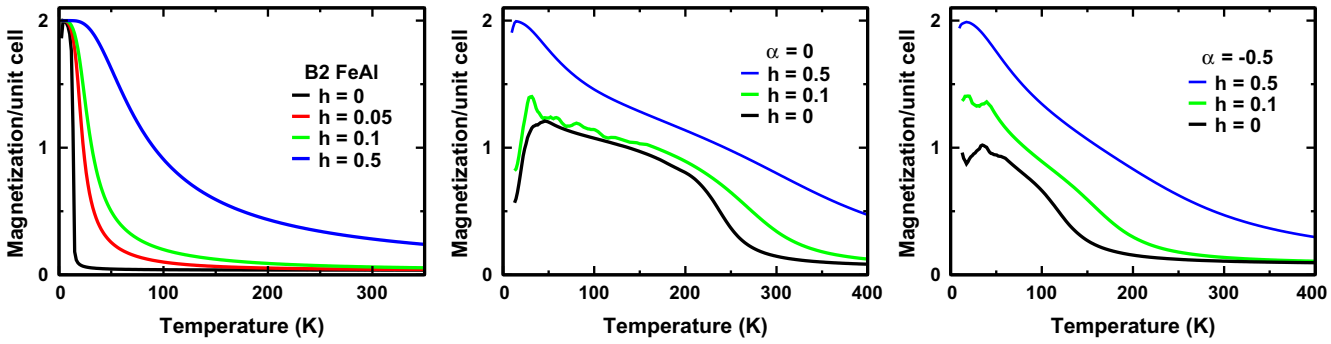

Fig. 7. Effect on magnetization of external magnetic field in an: (left) Ordered B2 structure, (center) a homogeneously disordered structure ($\alpha = 0$) and (right) a sample with short-ranged ordering $\alpha = -0.5$.

response of the ordered structure becomes the dominant contribution as can be seen from the left panel of Fig. 7 and both the homogeneously and inhomogeneously disordered structures behave in the same way. Though, at much lower fields the spin freezing temperature decreases as the external field increases similar to a canonical metallic spin glass, higher magnetic field suppresses the spin glass phase as expected. However, the magnetic state around this freezing temperature is quite complex due to the interplay between the magnetization of ordered B2 FeAl phase and the spin glass phase.

4. Conclusion

In this work we have revisited the 50–50 FeAl alloy both experimentally and theoretically in order to understand the often contradictory results quoted by different groups. Our conclusion is that inhomogeneous disorder seems to be inherent in the alloy and the magnetic behavior of the alloy is sensitive to chemical short-ranged ordering. Thus it is not surprising that alloys with different preparation conditions may exhibit different results. The magnetic behavior of this alloy is also very sensitive to the external magnetic field. The overall magnetic behavior seemed rather complex due the presence of short-ranged ordering, however, with a theoretical work we have established individual magnetic phases and their temperature behavior in detail.

Acknowledgment

One of us, APJ would like to thank the CSIR, India for financial support during this work.

References

[1] M. Besnus, A. Herr, A. Meyer, J. Phys. F: Met. Phys. 5 (1975) 2138.
[2] G. Huffman, R. Fisher, J. Appl. Phys. 38 (1967) 735–742.
[3] J. Bogner, W. Steiner, M. Reissner, P. Mohn, P. Blaha, K. Schwarz, R. Krachler, H. Ipser, B. Sepiol, Phys. Rev. B 58 (1998) 14922–14933.
[4] A.V. Smirnov, W.A. Shelton, D.D. Johnson, Phys. Rev. B 71 (2005) 064408.
[5] P. Mohn, C. Persson, P. Blaha, K. Schwarz, P. Novák, H. Eschrig, Phys. Rev. Lett. 87 (2001) 196401.
[6] S.K. Bose, V. Drchal, J. Kudrnovský, O. Jepsen, O.K. Andersen, Phys. Rev. B 55 (1997) 8184–8193.
[7] G. Caskey, J. Franz, S. Sellmyer, J. Phys. Chem. Solids 34 (1973) 1179–1198.
[8] H. Domke, L. Thomas, J. Magn. Magn. Mater. 45 (1984) 305–308.
[9] Y. Gu, L. Fritsche, J. Phys.: Condens. Matter 4 (1992) 1905.
[10] M. Shiga, Y. Nakamura, J. Phys. Soc. Jpn. 40 (1976) 1295–1299.
[11] N.I. Kulikov, A.V. Postnikov, G. Borstel, J. Braun, Phys. Rev. B 59 (1999) 6824–6833.
[12] P.G. Alcazar, E.G. daSilva, J. Phys. F: Met. Phys. 17 (1987) 2323.
[13] P. Shukla, M. Wortis, Phys. Rev. B 21 (1980) 159–164.
[14] K. Sumiyama, Y. Hirose, Y. Nakamura, J. Phys. Soc. Jpn. 59 (1990) 2963–2970.
[15] K. Szymaski, D. Satuła, L. Dobrzyski, E. Voronina, E.P. Yelsukov, T. Miyanaga, Phys. Rev. B 72 (2005) 104409.
[16] E. Yelsukov, E. Voronina, V. Barinov, J. Magn. Magn. Mater. 115 (1992) 271–280.
[17] R. Brajpuriya, P.P. Sharma, S. Jani, S. Kaimal, T. Shripathi, N. Lakshmi, K. Venugopalan, Appl. Surf. Sci. 257 (2010) 10–16.
[18] E. Apianiz, J. Garitaonandia, F. Plazaola, J. Non-Cryst. Solids 287 (2001) 302–307.
[19] L.E. Zamora, G.A. Pérez Alczar, G.Y. Vlez, J.D. Betancur, J.F. Marco, J.J. Romero, A. Martnez, F.J. Palomares, J.M. Gonzlez, Phys. Rev. B 79 (2009) 094418.
[20] S. Gialanella, X. Amils, M. Bar, P. Delcroix, G.L. Car, L. Lutterotti, S. Suriach, Acta Mater. 46 (1998) 3305–3316.
[21] N. Burke, Surf. Sci. 58 (1976) 349–373.
[22] P.K. Mukhopadhyay, T. Ghosh, A. Mookerjee, Phys. B: Condens. Matter. doi:http://dx.doi.org/10.1016/j.physb.2014.03.041.
[23] S. Radha, A. Nigam, S. Malik, G. Chandra, J. Magn. Magn. Mater. 140 (1995) 101–102.
[24] O.K. Andersen, O. Jepsen, Phys. Rev. Lett. 53 (1984) 2571–2574.
[25] A. Mookerjee, J. Phys. C: Solid State Phys. 6 (1973) 1340.
[26] A. Mookerjee, J. Phys. C: Solid State Phys. 6 (1973) L205.
[27] S. Ghosh, P.L. Leath, M.H. Cohen, Phys. Rev. B 66 (2002) 214206.
[28] R. Mills, P. Ratanavararaksa, Phys. Rev. B 18 (1978) 5291–5308.
[29] T. Saha, I. Dasgupta, A. Mookerjee, J. Phys.: Condens. Matter 6 (1994) L245.
[30] A. Zunger, S.-H. Wei, L.G. Ferreira, J.E. Bernard, Phys. Rev. Lett. 65 (1990) 353–356.
[31] I. Masanskii, V. Tokar, Theor. Math. Phys. 76 (1988) 747–757.
[32] V. Tokar, I. Masanskii, T. Grishchenko, J. Phys.: Condens. Matter 2 (1990) 10199.
[33] F. Ducastelle, F. Gautier, J. Phys. F: Met. Phys. 6 (1976) 2039.
[34] R.K. Chouhan, A. Mookerjee, J. Magn. Magn. Mater. 323 (2011) 868–873.
[35] J. von Pezold, A. Dick, M. Friák, J. Neugebauer, Phys. Rev. B 81 (2010) 094203.